

# Recent Warming Reverses Long-Term Arctic Cooling

## 2 Supporting Online Material

Notes A, B, C, D, and E

## 4 Figs. S1, S2, and S3

Tables S1 and S2

## 6 References

8 **Note A.** To avoid replication of records from closely spaced sites, we selected one of the two ice  
cores from central Greenland (GRIP rather than GISP2), and one of the two tree-ring records  
10 from southern Alaska (*S1*), which is based on regional curve standardization (rather than *S2*).  
None of the tree-ring records from Mann *et al.* (*S3*) fit the criteria for this synthesis because the  
12 first year with at least eight samples for each series was during the second millennium AD. We  
excluded the isotope-based records from ices cores in the Saint Elias Mountains (*S4*) and from  
14 Jellybean Lake carbonate (*S5*), both in the Yukon, because the proxies are more strongly  
controlled by changes in moisture-source and atmospheric moisture transport patterns than by  
16 temperature. Proxy values for five of the records include some interpolated values ( $n = 90$  total;  
Table S2).

18

**Note B.** To determine whether our network of sites accurately represents the observed Arctic-  
20 wide mean temperature, we used the gridded data from ERA-40 (*S6*) to obtain the monthly  
temperature at each of the proxy-record sites from 1958-2001. We focused on the June through  
22 August (JJA) mean temperature because the proxies are most strongly influenced by summer  
conditions. Between 1958 and 2001, the mean JJA temperature at the 23 proxy sites closely

24 tracked the mean JJA temperature from the ERA-40 data north of 60°N latitude ( $r^2 = 0.69$ ,  $p <$   
0.01) (Fig. S1). The average Arctic-wide warming trend between 1958 and 2001 was  $0.11 \pm$   
26  $0.07^\circ\text{C}$  per decade for the ERA-40 dataset compared with  $0.17 \pm 0.08^\circ\text{C}$  per decade at the proxy  
sites. The lake sites ( $n = 12$ ) are distributed more broadly and represent the average Arctic  
28 temperatures better than the ice ( $n = 7$ ) or tree ( $n = 4$ ) sites (Fig. S1).

Because summer temperatures track annual temperatures (Fig. S2), the inferences based  
30 on summer proxies also apply approximately to the mean annual temperature. During recent  
decades, warming has been stronger during the winter than during the summer. The CRUTEM3  
32 data (S7) show that summer trends are about 25-40% less than annual trends depending on the  
time period. For example, between 1976 and 2000, land areas north of 60°N latitude warmed by  
34  $0.30^\circ\text{C}$  per decade during the summer compared with  $0.40^\circ\text{C}$  per decade annually.

36 **Note C.** The annual proxy values shown in Manuscript Fig. 2 are from the ten sites with annually  
resolved data that extend through the 20<sup>th</sup> century (indicated in Table S1; the ten records contain  
38 a total of 28 missing annual values). They were standardized to a mean of zero and unit variance.  
The 10-year-mean proxy values (bold red line in Manuscript Fig. 2) are based on the 19 sites that  
40 extend into the late 20<sup>th</sup> century (Table S1). Nine of the 19 records contain one or two missing  
values (Table S2). The 10-year-mean values were standardized using a reference period of 980 to  
42 1800 AD, the period common to all of the proxy records. These 10-year averages were used to  
develop the least-squares regression equation that scales temperature (independent variable) to  
44 the standardized proxy value (Fig. S3). The equation is:

$$P = 2.079T + 0.826 \quad (r^2 = 0.79, p < 0.01, n = 14)$$

46

where  $T$  is the 10-year average Arctic-wide summer (JJA) temperature anomaly relative to 1961-  
48 1990, and  $P$  is the 10-year average proxy value (SD units). The 95% confidence interval on the  
slope of the regression is  $\pm 0.89 \text{ SD } ^\circ\text{C}^{-1}$  (SOM note D). Spearman's ranked correlation  
50 coefficient  $r_s = 0.88$ , nearly identical to Pearson's ( $r = 0.89$ ), indicating that the regression is  
robust. Note that the annual proxy values (narrow red line) were shifted upward by 0.6 SD so  
52 that they overlapped the 10-year-average values. This accounts for difference in the reference  
periods used for the annual versus the 10-year-average values, and improves the visual  
54 presentation, but did not enter into the scaling procedure.

56 **Note D.** Throughout this paper, we used the “adjusted standard error + adjusted degrees of  
freedom” procedure to assess the significance of all of the trends calculated by least-squares  
58 linear regression (S8), where the effective number of samples is estimated from the lag-1  
autocorrelation of the regression residuals, as shown in the example of supporting ref 8. The 95%  
60 confidence interval was calculated as the adjusted standard error times the adjusted critical  $t$ -  
value from a two-tailed  $t$ -test. For the  $t$ -test of the correlation coefficients reported in the text, we  
62 also reduced the number of degrees of freedom, according to the formula:

$$n^* = (n - 2) [(1 - r_1^2) / (1 + r_1^2)]$$

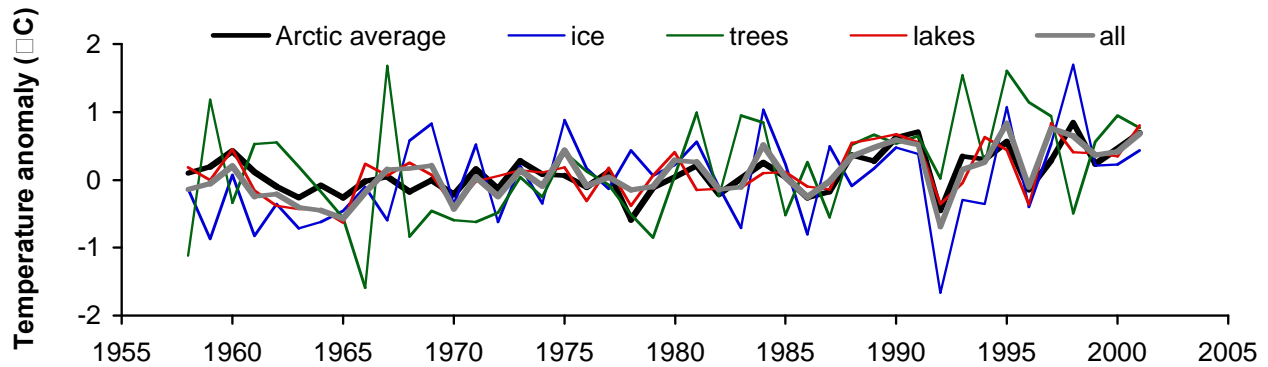
64 where  $n$  = original sample size;  $n^*$  = adjusted sample size;  $r_1$  = lag-1 correlation coefficient of  
the two time series being compared. This was then used in a two-tailed  $t$ -test and compared with  
66 the critical  $t$ -value.

**Note E.** The Community Climate System Model, version 3 (CCSM3) is a global coupled  
68 atmosphere, ocean, sea-ice, and land model. An overview of the model is provided by Collins *et*

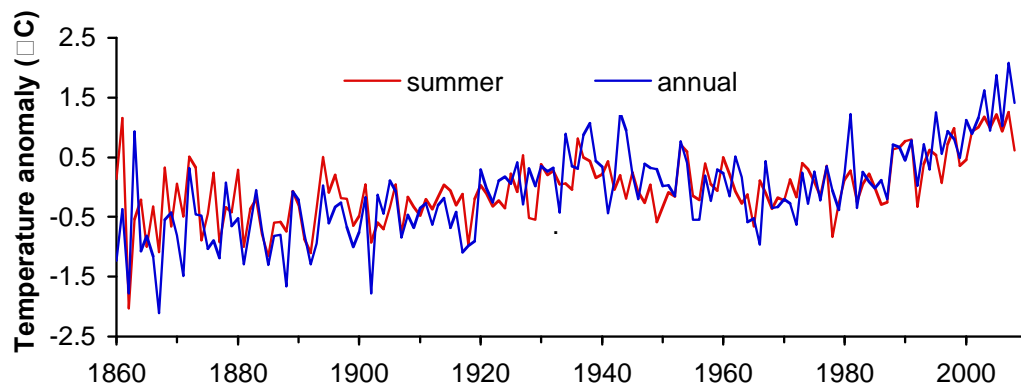
70 *al.* (S9). The simulation used for this data-model comparison was conducted with a configuration  
of the atmosphere and land component models on a 3.8° X 3.8° latitude-longitude grid and the  
ocean and sea-ice models on a roughly 3° X 3° horizontal grid, with higher resolutions in the  
72 tropics and North Atlantic. The atmosphere, with a spectral dynamical core (T31), has 26 levels  
in the vertical. The climate sensitivity of this low-resolution version of the CCSM3 is discussed  
74 in Otto-Bliesner *et al.* (S10). Vegetation is allowed to change dynamically with the climate  
(S11).

76 The length of the simulation was 2400 years, corresponding to 4050 to 1650 BC. The  
time period analyzed here is the 2000-year period from 3650 to 1650 BC. No similar simulation  
78 with orbital forcing is available for the most recent two millennia covered by the proxy records.  
However, boundary conditions were similar to the preindustrial (PI) period. In this simulation,  
80 ozone, tropospheric sulfates, dust, sea salt, and carbonaceous aerosols were set to the same  
values as in the PI control simulation (S10), which served as this simulation's initial conditions.  
82 Time-varying forcings included concentrations of greenhouse gases (CO<sub>2</sub>, CH<sub>4</sub>, N<sub>2</sub>O), solar  
irradiance, volcanism, and changes in insolation due to orbital variations. Estimates of global  
84 greenhouse gas concentrations come from measurements of trapped gases in ice cores, as used  
for the mid-Holocene simulation by Otto-Bliesner *et al.* (S12), while solar irradiance is inferred  
86 from the ice-core isotope proxies, <sup>10</sup>Be and <sup>14</sup>C (R. Muscheler, pers. commun., 2005). The mean  
solar constant is 1365.7 Wm<sup>-2</sup>, similar to the value used for the PI control, and the amplitude of  
88 long-term changes are on the smaller side of the range of estimates (S13). Perturbations from  
volcanism were estimated statistically, based on the magnitude, frequency, and location of  
90 eruptions in the period 850 to 2000 AD. All of these time-varying forcings had little impact  
compared with the orbital forcing; over the period 3650 to 1650 BC, CO<sub>2</sub> increased from about

92 265 to 271 ppm<sub>v</sub>, CH<sub>4</sub> remained close to 580 ppb<sub>v</sub>, and N<sub>2</sub>O remained close to 261 ppb<sub>v</sub>. Solar  
irradiance and volcanism also had only small changes. Unlike the other forcings, orbital forcing  
94 can be precisely calculated (*S14*). At 65°N, summer (JJA) insolation decreased by about 7.1 Wm<sup>-2</sup>  
<sup>2</sup> during the modeled period 3650 to 1650 BC. This provides a basis for calculating the  
96 sensitivity of Arctic land temperature to orbital forcing (Manuscript Fig. 4B), and comparison  
with the proxy-inferred sensitivity (Manuscript Fig. 4A).

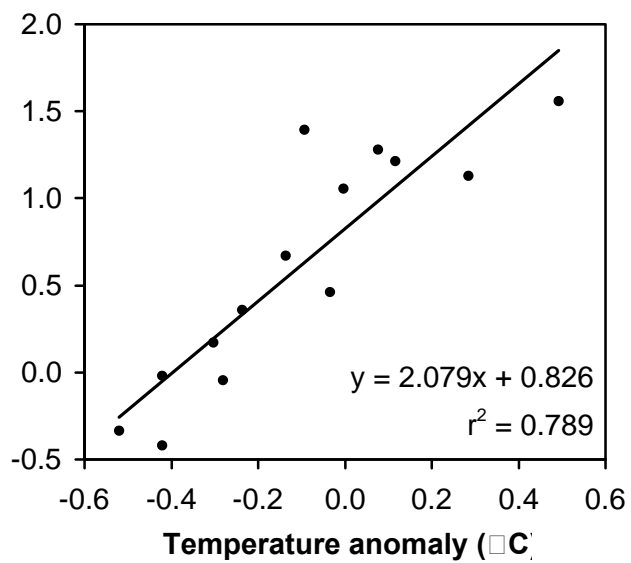


100 **Fig. S1.** Comparison of the Arctic-wide mean summer (JJA) temperature (land area north of 60°  
 102 latitude relative to 1961-1990) with the temperature at the 23 proxy sites, subdivided by proxy  
 104 type. Between 1958 and 2001, the mean JJA temperature at location of each of our 23 proxy sites  
 combined (grey line) closely tracked the Arctic-wide average ( $r^2 = 0.69$ ,  $p < 0.01$ ). Data are from  
 the ERA-40 gridded dataset (S6) and evaluated annually from 1958-2001. Site locations and  
 proxy types are shown in Manuscript Fig. 1.



106

**Fig. S2.** Comparison of the Arctic-wide (land area north of 60°N latitude) mean summer (JJA) and annual temperature anomalies (relative to 1961-1990). Data are from the CRUTEM3 dataset (S7) relative to the 1961-1990 mean.



110

**Fig. S3.** Relation used to scale proxy values to summer temperature (SOM note C). The 10-year-

112 mean proxy values are based on the 19 sites that extend to the late 20<sup>th</sup> century (Table S1).

Temperatures are Arctic-wide, June through August (JJA), 10-year means from the CRUTEM3

114 dataset (S7) relative to the 1961-1990 mean.



116 **Table S1.** Paleoclimate proxy records included in this synthesis listed from west to east.

Map no.	Site name	General location	Proxy type*	PC1 r-value	Length (AD)†	Source
1	Blue Lake	N Alaska	Varves - thickness	-	730 - <b>2000</b>	Bird <i>et al.</i> (S15)
2	Hallet Lake	Alaska	Sediment - BSi	0.44	1 - 2000	McKay <i>et al.</i> (S16)
3	Gulf of Alaska	S Alaska	Tree rings (RCS)	-	720 - <b>2000</b>	D'Arrigo <i>et al.</i> (S1)
4	Iceberg Lake	Alaska	Varves - thickness	-	460 - <b>2000</b>	Loso (S17)
5	Devon Ice Cap	Devon Is	Ice - isotopes	0.61	1 - 1980	Fisher (S18)
6	Lake C2	Ellesmere Is	Varves	-	1 - <b>2000</b>	Lamoureaux & Bradley (S19)
7	Agassiz Ice Cap	Baffin Island	Ice - isotopes	0.49	1 - 1980	Vinther <i>et al.</i> (S20)‡
8	Lower Murray Lake	Ellesmere Is	Varves	0.10	1 - 2000	Cook <i>et al.</i> (S21)
9	Big Round Lake	Baffin Is	Varves	-	980 - <b>2000</b>	Thomas & Briner (S22)
10	Donard Lake	Baffin Island	Varves	-	750- <b>2000</b>	Moore <i>et al.</i> (S23)
11	SFL4	W Greenland	Sediment - OM	0.67	1 - 1940	Willemse & Törnqvist (S24)
12	DYE-3	S Greenland	Ice - isotopes	0.44	1 - 1980	Andersen <i>et al.</i> (S25) ¶
13	NGRIP	N Greenland	Ice - isotopes	0.42	1 - <b>2000</b>	NGRIP members (S26) ‡
14	GRIP	Central Greenland	Ice - isotopes	0.41	1 - 1990	Johnsen <i>et al.</i> (S27)
15	Crete	Central Greenland	Ice - isotopes	-	550 - 1980	Clausen <i>et al.</i> (S28)
16	Renland	SE Greenland	Ice - isotopes	0.49	1 - 1990	Vinther <i>et al.</i> (S20)‡
17	Haukadalsvatn	SW Iceland	Sediment - BSi & OM	0.38	1 - 2000	Geirsdóttir <i>et al.</i> (S29)
18	Fennoscandia	Fennoscandia	Tree rings	0.17	1 - <b>2000</b>	Briffa <i>et al.</i> (S30)
19	Lake Nautajärvi	Finland	Varves - organic content	-	1 - 1800§	Ojala <i>et al.</i> (S31)
20	Lake Korttajärvi	Finland	Varves - X-ray density	-	1 - 1800§	Tiljander <i>et al.</i> (S32)
21	Lake Lehmilampi	Finland	Varves- thickness Tree rings	0.07 0.22	1 - 1950§ 1 - <b>2000</b>	Haltia-Hovi <i>et al.</i> (S33)
22	Yamal	NW Siberia	Tree rings	0.16		Briffa <i>et al.</i> (S30)
23	Avam-Taimyr	Siberia			1 - <b>2000</b>	Briffa <i>et al.</i> (S30)

118

\*BSi — biogenic silica content; OM — organic matter content.

120 †Rounded to nearest decade; bold **2000** — ten records that are annually resolved through the 20<sup>th</sup> century (Manuscript Fig. 2).

122 ‡Published data are smoothed at 20 years; our synthesis is based on unpublished annually resolved data provided by BMV.

124 ¶ The oxygen-isotope values from DYE-3 were corrected to account for the flow of ice from higher elevation. Using an ice-flow model for the area (S34), we determine the relation between the change in the depositional elevation of the snow and the age of ice (0.035 m yr<sup>-1</sup>). Combining this with the Greenland isotope-elevation gradient of -0.006‰ m<sup>-1</sup> (S35), a correction of 0.00021‰ yr<sup>-1</sup> was derived for the DYE-3 isotope time series.





136 **References for SOM**

1. R. D'Arrigo, R. Wilson, G. Jacoby, *J. Geophys. Res.* **111**, D03103 (2006).
- 138 2. R. Wilson, G. Wiles, R. D'Arrigo, C. Zweck, *Clim. Dyn.* **28**, 425 (2007).
3. M. E. Mann *et al.*, *Proc. Nat. Acad. Sci.* **105**, 13252 (2008).
- 140 4. D. A. Fisher *et al.*, *Holocene* **18**, 667 (2008).
5. L. Anderson, M. B. Abbott, B. P. Finney, S. J. Burns, *Quat. Res.* **64**, 21 (2005).
- 142 6. <http://dss.ucar.edu/pub/era40/>
7. Climate Research Unit CRUTEM3 temperature data described by P. Brohan, J. J. Kennedy,  
144 I. Harris, S. F. B Tett, P. D. Jones, *J. Geophys. Res.* **111**, D12106 (2006), and available at:  
<http://www.cru.uea.ac.uk/cru/data/temperature/>
- 146 8. B. D. Santer *et al.*, *J. Geophys. Res.* **105**, 7337 (2000).
9. W. D. Collins *et al.*, *J. Clim.* **19**, 2122 (2006).
- 148 10. B. L. Otto-Bliesner, R. Tomas, E. C. Brady, C. Ammann, Z. Kothavala, G. Clauzet, *J. Clim.*  
**19**, 2567 (2006).
- 150 11. S. Levis, G. B. Bonan, M. Vertenstein, K. W. Oleson, *The Community Land Model's*  
*dynamic global vegetation model (CLM-DGVM): Technical description and user's guide.*  
152 NCAR Tech. Note TN-549+IA (2004).
12. B. L. Otto-Bliesner, E. C. Brady, G. Clauzet, R. Tomas, S. Levis, Z. Kothavala (2006b), *J.*  
154 *Clim.* **19**, 2526 (2006).
13. C. M. Ammann, F. Joos, D. S. Schimel, B. L. Otto-Bliesner, R. A. Tomas, *Proc. Natl. Acad.*  
156 *Sci.* **104**, 3713 (2007).
14. A. Berger, M. F. Loutre, *Quat. Sci. Rev.* **10**, 297 (1991).
- 158 15. B. W. Bird, M. B. Abbott, B. P. Finney, B. Kutchko, *J. Paleolimnol.* **41**, 25 (2009).
16. N. P. McKay, D. S. Kaufman, N. Michelutti, *Geophys. Res. Lett.* **35**, GL032876 (2008).

- 160 17. M. Loso, *J. Paleolimnol.* **41**, 117 (2009).
18. D. A. Fisher, *Quat. Res.* **11**, 299 (1979).
- 162 19. S. F. Lamoureux, R. S. Bradley, *J. Paleolimnol.* **16**, 239 (1996).
20. B. M. Vinther *et al.*, *J. Geophys. Res.* **112**, D08115 (2008).
- 164 21. T. L. Cook, R. S. Bradley, J. S. Stoner, P. Francus, *J. Paleolimnol.* **41**, 77 (2009).
22. E. K. Thomas, J. P. Briner, *J. Paleolimnol.* **41**, 209 (2009).
- 166 23. J. J. Moore, K. A. Huguen, G. H. Miller, J. T. Overpeck, *J. Paleolimnol.* **25**, 503 (2001).
24. N. W. Willemsen, T. E. Törnqvist, *Geology* **27**, 580 (1999).
- 168 25. K. K. Andersen, P. D. Ditlevsen, S. O. Rasmussen, H. B. Clausen, B. M. Vinther, S. J. Johnsen, *J. Geophys. Res.* **111**, D15106 (2006).
- 170 26. North Greenland Ice Core Project members, *Nature* **43**, 147 (2005).
27. S. J. Johnsen *et al.*, *J. Geophys. Res.* **102**, 26397 (1997).
- 172 28. H. B. Clausen *et al.*, *Ann. Glaciol.* **10**, 10 (1988).
29. Á. Geirsdóttir, G. H. Miller, T. Thordarson, K. B. Ólafsdóttir, *J. Paleolimnol.* **41**, 95 (2009).
- 174 30. K. R. Briffa *et al.*, *Phil. Trans. R. Soc. B* **363**, 2269 (2008).
31. A. E. K. Ojala, T. Alenius, H. Seppä, T. Giesecke, *Holocene* **18**, 529 (2008).
- 176 32. M. Tiljander, J. A. Karhu, T. Kauppila, *J. Paleolimnol.* **36**, 233 (2006).
33. E. Haltia-Hovi, T. Saarinen, M. Kukkonen, *Quat. Sci. Rev.* **26**, 678 (2007).
- 178 34. N. Reeh *et al.*, *Am. Geophys. Union Geophys. Mono.* **33**, 57 (1985).
35. W. Dansgaard, *Medd. Grønland* **165**(2) (1961).